HHS Public Access

Author manuscript

Acta Biomater. Author manuscript; available in PMC 2016 May 01.

Published in final edited form as:

Acta Biomater. 2015 May ; 18: 30–39. doi:10.1016/j.actbio.2015.02.005.

Highly Elastic and Suturable Electrospun Poly(Glycerol Sebacate) Fibrous Scaffolds

Eric M. Jeffries, **Robert A. Allen**, **Jin Gao**, **Matt Pesce**, and **Yadong Wang**

Departments of Bioengineering, Chemical and Petroleum Engineering, Surgery, Mechanical Engineering and Materials Science, and the McGowan Institute for Regenerative Medicine, 3700 O'Hara Street, 411 Benedum Hall, Pittsburgh, PA 15261, USA.

Abstract

Poly(glycerol sebacate) (PGS) is a thermally-crosslinked elastomer suitable for tissue regeneration due to its elasticity, degradability, and pro-regenerative inflammatory response. Pores in PGS scaffolds are typically introduced by porogen leaching, which compromises strength. Methods for producing fibrous PGS scaffolds are very limited. Electrospinning is the most widely used method for laboratory scale production of fibrous scaffolds. Electrospinning PGS by itself is challenging, necessitating a carrier polymer which can affect material properties if not removed. We report a simple electrospinning method to produce distinct PGS fibers while maintaining the desired mechanical and cytocompatibility properties of thermally crosslinked PGS. Fibrous PGS demonstrated 5 times higher tensile strength and increased suture retention compared to porous PGS foams. Additionally, similar modulus and elastic recovery were observed. A final advantage of fibrous PGS sheets is the ability to create multi-laminate constructs due to fiber bonding that occurs during thermal crosslinking. Taken together, these highly elastic fibrous PGS scaffolds will enable new approaches in tissue engineering and regenerative medicine.

Keywords

Electrospinning; fiber; poly (glycerol sebacate) (PGS); poly (vinyl alcohol) (PVA); elastomer

1. Introduction

Scaffold mechanical properties play an important role in the cellular microenvironment, influencing cell motility, organization, and differentiation [1, 2]. Traditional plastic biomaterials- (poly(caprolactone) (PCL), poly(glycolic acid) (PGA), poly(lactic acid) (PLA)) [3] as well as elastomeric biomaterials- (poly(ether urethane urea) (PEUU), poly(3-hydroxybutyrate-co-4-hydroxybutyrate) (P3HB-co-P4HB), and poly(caprolactone-co-lactic acid) (PCL-co-LA)) [4] have moduli in the MPa-GPa range. In contrast poly(glycerol

yaw20@pitt.edu, Phone: 412-624-7196, Fax: 412-524-3699.

sebacate) (PGS) is a soft elastomer with a modulus between 0.025-1.2 MPa depending on crosslinking density [5]. This makes PGS a unique and desirable material for engineering soft tissues including vascular [6-8], cardiac [9-11], neural [12], and ocular [13] which have moduli between 0.1-11.1 MPa when measured by tensile methods [14]. Additionally, PGS degrades rapidly *in vivo* into glycerol and sebacic acid, metabolites naturally exist in the body, minimizing the duration of host inflammatory response [5, 15].

The application of porous PGS scaffolds has been limited by their need for gentle handling. The low tensile strength of scaffolds produced by solvent casting porogen leaching precludes their use in load bearing environments or implants requiring suture anchoring. [16, 17] Porogen leached PGS can be composited with a stronger material to improve surgical handling [6], but the additional material will influence the overall mechanical behavior and degradation of the implant.

Constructing fibrous scaffolds by electrospinning can improve the strength of PGS scaffolds [18] while introducing a fibrous topography that resembles the structure of extracellular matrix [19]. This is because pores can be considered to be mechanical defects whereas fibers are known to provide tensile strength. Electrospinning thermosets like PGS is challenging [20] for two reasons: (1) The insolubility of crosslinked PGS in organic solvents necessitates the use of the uncrosslinked PGS prepolymer (pPGS); and (2) pPGS has a glass transition temperature (Tg) below room temperature causing the polymer to flow and fibers fuse into a nonporous sheet. This fusion is exacerbated by the high temperature needed for thermal crosslinking.

To overcome these challenges, we and others have developed a range of methods to electrospin PGS (Table 1). All of these techniques blend pPGS with a carrier polymer that readily forms fibers to facilitate fiber formation. Unfortunately, if the carrier polymer is not removed or if pPGS is not crosslinked, the properties of the PGS scaffold would differ substantially from those of unaltered PGS [15]. We developed a simple and low cost method for electrospinning PGS scaffolds that retains the mechanical properties of crosslinked PGS without using toxic crosslinkers or organic solvents to remove the carrier. We chose poly(vinyl alcohol) (PVA) as the carrier because (1) it does not melt during thermal crosslinking, and (2) it is highly water-soluble, enabling safe removal by dissolution in water. Additionally, PVA is a nontoxic and noncarcinogenic biomaterial. It is approved by the US Food and Drug Administration for applications in food chemistry and pharmaceuticals, [21] and is also being investigated for use in contact lenses, wound dressing, coatings for sutures and catheters, and other tissue engineered scaffolds [21, 22]. The results described here demonstrated that we have overcome the challenge of electrospinning and thermally crosslinking PGS.

2. Materials and methods

2.1 Materials

Poly(vinyl alcohol) (PVA) was generously provided by Soarus LLC (Arlington Heights, IL) and 1,1,1,3,3,3-hexafluoroisopropanol (HFIP) was purchased from Oakwood Products Inc.

(West Columbia, SC). PGS prepolymer (pPGS) was synthesized in house as previously described [15].

2.2 Production of fibrous PGS sheets

Fibrous PGS sheets were fabricated by 1) electrospinning pPGS-PVA blends, 2) thermal crosslinking, and 3) purifying with water and ethanol as outlined in **Figure 1**. A 16 w/v% solution was prepared by mixing pPGS and PVA at 55:45 mass ratio and dissolving in HFIP overnight. This solution was pumped at 29 μL/min through a 22 gauge needle serving as the spinneret. Positive and negative 9 kV were applied to the spinneret and another needle positioned 60cm from the spinneret, respectively. Electrospun fibers were collected on a rotating aluminum mandrel (100RPM) placed between the needles at a 30 cm distance from the spinneret **(Figure 1-1)**. No voltage was placed on the mandrel.

Fibrous sheets were removed from the collector and crosslinked in a preheated vacuum oven under high temperature (120°C-150°C) and vacuum (60 mm Hg) **(Figure 1-2)**. We investigated crosslinking at 120°C for 24h (**C1**), 48h (**C2**), 72h (**C3**), and 96h (**C4**). As a means to achieve a high degree of crosslinking with less processing time, we also explored 120°C for 24h followed by 150°C for 24h (**C5**).

Crosslinked fibrous sheets were purified by water and ethanol washes **(Figure 1-3)**. PVA was removed by washing in ultrapure, deionized water (diH_2O) with gentle agitation for 24h. The water was changed after the first and second hours because of the large amount of PVA removed within this time as evident by the foamy water. Non-crosslinked pPGS was removed via serial ethanol washes (100%-1h, 70%-1h, 50%-15min, 25%-15min, diH_2O-15min three times) with gentle agitation. Hydrated samples were used immediately or lyophilized for storage.

2.3 Characterization of electrospun PGS sheets

Fiber morphology was evaluated by scanning electron microscopy (SEM). Samples were prepared for SEM by adhering onto aluminum stubs with conductive carbon tape before sputter coating with gold-palladium to a 3.5nm thickness and viewing on a JSM-6330F SEM (JEOL, Tokyo, Japan). Fiber diameter was measured by image analysis with ImageJ (NIH, Bethesda, MD).

Purification (removal of pPGS and PVA) was evaluated by mass loss. Dry samples were weighed on a microbalance before undergoing washing protocols. Sample thicknesses were also measured with dial calipers before and after purification. Fourier transform infrared attenuated total reflectance (ATR-FTIR) was measured on a Nicolet iS10 FTIR spectrometer (Thermo Scientific, Waltham, MA) after 1) electrospinning, 2) crosslinking, and 3) purification. Samples were compared to control films of pure PGS at the same crosslinking conditions. The thermal properties for the same groups were measured by differential scanning calorimetry (DSC, Q200, TA Instruments). Samples underwent two cycles of heating to 200°C and cooling to −80°C at 20°C/min.

2.4 Mechanical properties

Mechanical properties of electrospun PGS blends were measured by uniaxial tensile testing. Fully washed samples were cut into dog bone shaped test specimens using a customized punch with outer dimensions (28.75mm (L) * 4.75mm (W)) and a narrow region (8.25mm (L) * 1.5mm (W)). Sample thickness was measured by dial calipers. Samples were placed on a MTS Insight (Eden Prairie, MN) and then hydrated in diH_2O immediately before stretching to failure at 25 mm/min. Multi-cycle testing from 10 to 100% strain for 100 cycles at 100 mm/min was performed on hydrated samples to evaluate elastic recovery. Suture retention strength was measured by inserting a 4-0 suture 2mm from the edge of the long axis of 5mm × 20mm samples and strained to rupture. Suture retention strength was calculated as maximum load/(suture diameter × sample thickness) in N/mm^2.

2.5 Cell attachment and viability

Purified and unpurified samples of electrospun PGS sheets crosslinked at medium and high conditions were autoclaved at 121°C for 27min. Fiber morphology of autoclaved PGS sheets was observed via SEM **(Figure 2*).**

Extract Tests with 3T3 cells (Live/Dead)—Cytocompatibility was performed according to the ISO 10993-5 standard for extract tests. Autoclaved disks were incubated in media at 20 g/mL overnight at 37°C. 3T3 fibroblasts were plated in a 96-well plate at 10,000 cells per well for 3h before incubating with the extract at 1 and 10mg/mL for 24h. Cells were incubated with methanol overnight as a positive control for cytotoxicity. Cells were incubated with serum-free medium with 2μM calcein AM and 4 μM ethidium homodimer for one half hour before capturing FITC and TRITC images at the center of each well (n=3 for each sample) with Nikon Eclipse T*i* microscope. Live and dead cell numbers were quantified using “object count” in Nikon Elements software to threshold images and exclude objects less than 10μm. Live percent was calculated as the number of live cells/total cells × 100. Since all wells contained some dead cells, the live percent was normalized to controls grown on tissue culture polystyrene (TCPS) with no extract.

3T3 Cells on PGS (Live/Dead & SEM)—Washed PGS sheets (1.2cm diameter) were placed under stainless steel rings in 12-well plates such that the samples were fully immersed in media (DMEM + 10% FBS +1% antibiotic) and incubated for 24h. The incubation media was removed and 3T3 fibroblasts were seeded at 10,000 cells per well and cultured for 24h. Cell viability was assessed by Live/Dead assay (Molecular Probes, Eugene, OR) using fluorescent imaging. Replicates were fixed in 2.5% glutaraldehyde before dehydrating with a series of ethanol, followed by hexamethyldisilazane (HMDS, Alfa Aesar, Ward Hill, MA). Cell attachment was examined by SEM.

Human cord blood endothelial cells (hcbEC) on PGS (CellTiter-Blue Cell Viability)—Fibrous poly(lactic-co-glycolic acid) (PLGA) 5050DLG9A (Evonik, Essen Germany) was electrospun and used as a positive control. Briefly, a 15% solution of PLGA in HFIP was electrospun onto an aluminum plate collector at a distance of 30 cm, 11μL/min flow rate, and 7 kV+ and kV− potential. Disks (1.2 cm diameter) of PLGA and purified PGS fibrous sheets were prepared and sterilized by 70% ethanol and ultraviolet exposure for 30

minutes. Samples were placed in 12 well plates under stainless steel rings and incubated at 37°C overnight in endothelial growth media EGM-2 BulletKit (Clonetics). Primary human cord blood endothelial cells (P9) were seeded onto PGS, PLGA, and fibronectin-coated (7.8 μg/mL) tissue culture polystyrene (TCPS) wells at 50,000 cells per well. Cells were cultured for 1, 3, and 7 days at 37 °C before measuring cell viability by CellTiter-Blue colorimetric assay. Briefly, CellTiter-Blue solution was combined with EGM culture media at 1:5 volumetric ratio and incubated with the samples for 4 hours at 37°C. Fluorescence was measured in triplicate for each group (n = 3) at 560 / 590 nm excitation/emission using a Biotek SynergyMx plate reader. For negative controls, cells grown on TCPS were killed by 70% methanol for 0.5h before adding CellTiter-blue.

2.6 Subcutaneous Implantation

Disks of fibrous PGS and PLGA control were (4 mm diameter, 0.2-0.3 mm thickness) sterilized with ethylene oxide, washed three times with sterile 1X phosphate buffered solution (PBS) and implanted subcutaneously in C57BL/6 (Jackson Laboratory) adult mice. Samples explanted at 3 and 14 days were cryosectioned at 6 μm cross-sections and stained with hematoxylin and eosin (H&E) and Masson's trichrome. Evaluation of the cellular response was performed by a pathologist.

2.7 Tubular scaffolds

Tubular scaffolds were fabricated by electrospinning around various-sized mandrels coated with 1-2 w/v % hyaluronic acid and crosslinking and purifying as described above. Hyaluronic acid coating and drying of the coating were performed as previously described [8]. These tubular scaffolds had elastic recoil and resist kinking (**Supplementary video 2**).

2.8. Multi-laminate scaffolds

Thick scaffolds were constructed by stacking uncrosslinked pPGS-PVA fiber sheets between Teflon block as shown in **Figure 8a**. After C2 crosslinking, these scaffolds were purified by water and ethanol washes before lyophilizing as previously described. Bonding of the laminated layers was verified by delamination tests performed with stacked samples (2 separate sheets of pPGS-PVA fibers) and directly electrospun samples (the second sheet was electrospun onto the first). Parafilm sheets were placed between the sheets at one end of the sample to prevent bonding at that region and allow loading into the MTS grips. Lamination was performed at 120°C for 48h. Bonding was determined by performing the T-peel test on hydrated samples according to ASTM D1876-08.

2.9. Statistical analysis

ANOVA was performed in Minitab using the general linear model. Post-hoc comparisons with the control were performed using Bonferroni correction and 95% confidence interval. Data represent mean ± standard deviation.

3. Results and Discussion

3.1 Prior work

PGS is intrinsically difficult to electrospin [20, 23]. Existing literature pertaining to electrospun pPGS use a carrier polymer that is blended or electrospun by coaxial set-up (**Table 1**). PCL might not be a suitable carrier polymer since its low melting point prohibits thermal crosslinking to PGS, making PCL difficult to remove and alter the properties of the resultant scaffold. As a result, pPGS-PCL blends exhibit mechanical properties more similar to PCL than PGS [24]. Additionally, noncrosslinked pPGS may have a cytotoxic effect if pPGS is not removed from the scaffold [25]. Gelatin has been used as a carrier but it requires crosslinking methods that use glutaraldehyde, acrylate-ultraviolet (UV), or EDC-NHS, which may alter PGS structure and properties and trigger inflammation and calcification [26-28]. Coaxial electrospun pPGS-PLLA tolerated thermal crosslinking and removal of the PLLA sheath by dissolution in dichloromethane (DCM) [23]. However, DCM is toxic and a suspect carcinogen, requiring stringent and complete removal before biomedical applications. Our group has experienced similar challenges using a range of other carrier polymers (**Table 1**). PCL and PLGA carrier polymers melted during heating, poly(dioxanone) (PDO) and gelatin blends were severely weakened by heat, and poly(ethylene terephthalate) (PET) required purification using large quantities of toxic and costly HFIP to remove the carrier polymer. While we acknowledge that some PVA appears to be incorporated into the final fibers, our results suggest that PVA does not significantly affect mechanical properties or cytocompatibility (**Figures 4 & 5**).

3.2 Fiber morphology

PVA was blended with pPGS at a ratio of 45:55 to facilitate fiber formation. This ratio was determined empirically to minimize fiber fusion while maintaining scaffold mechanical integrity. Fiber fusion increased with greater pPGS content while higher PVA content caused rapid disintegration of the fibrous mat after PVA removal. Electrospinning this solution yielded uniform round fibers of 2.8 ± 1.2 μm diameter (**Figure 2a**) with fusion restricted to the contact points between fibers (**Figure 2b**). Prior work suggests that fibers of this diameter (2μm) may be beneficial for facilitating endothelial cell attachment in vascular applications [29]. However, application requirements may necessitate parameter adjustment to obtain larger or smaller diameters in the future. Collection around a rotating mandrel resulted in fibers oriented with circumferential preference. Randomly deposited fibers can also electrospun to a stationary plate (not shown), but were not characterized in this work which focuses on tissue engineering of tubular organs.

Maintaining the defined fibrous structure during thermal crosslinking was challenging since elevated temperatures causes pPGS to soften and fuse. To improve fiber quality and reduce fiber fusion, we tested three different pPGS-PVA mass ratios (60:40, 55:45, 50:50) in addition to ramped (4°C/h) and rapid (preheated) crosslinking conditions (**Figure S1**). Results indicate that a ratio of 55:45 pPGS:PVA is the best of the 3 ratios for fiber quality (**Figure S1)** and that ramped heating does not reduce fusion. The fibrous structure is retained during crosslinking although fiber fusion appears to increase with greater crosslinking (**Figure 2c-e**).

Water washing appears to have little effect on fiber morphology (**Figure 2f-h**) compared to the significant changes observed after ethanol washes (**Figure 2i-k**). High resolution images of the purified fibers show morphological changes as the degree of crosslinking is varied. Purified C1 fibers are irregularly-shaped and have small spines branching off each fiber (**Figure 2i**). Purified C2 and C5 fibers exhibit a semi-tubular shape with a hollow core (**Figure 2j**). Additionally, C5 fibers contain a porous nanostructure and some recession near the fusion points (**Figure 2k-arrowheads**). We believe that the non-uniformity arises due to mixing of the polymer blend and the semi-circular structure may result from the gravitational force acting on the pPGS during crosslinking, resulting in separate PGS and PVA domains. After dissolution, this separation is revealed by the hollow core. Furthermore, the short crosslinking time during C1 may not allow time for this PGS-PVA separation to occur.

While the processing of thermosets is difficult, their resistance to heat and solvents is beneficial for sterilization. Many common degradable polyesters (PCL, PLGA, and PDO) have low melting points and cannot be autoclaved. Although autoclaving affects the fiber morphology, we demonstrate that purified PGS can be autoclaved without loss of the fibrous structure (**Figure 2j*&k***). A significant amount of uncrosslinked pPGS remains in the C1 sample (**Figure S2**) and is fluid enough to fill in pores during autoclaving. This causes unpurified C1 fibers (**Figure 2d*)** to appear fused while the purified sample (**Figure 2j***) clearly shows the fibrous structure after pPGS removal. Since a greater percentage of the pPGS is crosslinked to thermoset PGS in the C5 group (**Figure S2**), the fibrous structure is evident in both unpurified (**Figure 2e***) and purified (**Figure 2k***) samples for this group.

3.3 Analysis of fiber composition

After water washing, all samples had greater than 55% mass remaining, which was the percentage of pPGS in the original solution **(Figure 3a)**. After ethanol washing, the C1 and C2 were the only groups with less than 55% mass remaining **(Figure 3a)**. Mass loss during the water wash likely represents PVA removal due to its high solubility in water. Since both pPGS and PVA are soluble in ethanol, mass loss during the ethanol wash should include pPGS and PVA that was physically entangled within it. From this mass balance, we conclude that the three most crosslinked groups (C3-C5) have some residual PVA in the final product. Although C1 and C2 show less than 55% mass remaining, purification of PGS films **(Figure S2)** suggests that these crosslinking conditions may leave 20-34% of the pPGS uncrosslinked. Thus, it is possible that removing this large amount of pPGS conceals the mass from any residual PVA. The most likely scenario for residual PVA to occur is via physical entanglement within PGS fibers. Other possibilities involve PVA becoming insoluble as a result of thermal treatment [22] or chemically crosslinking with PGS by condensation reactions with residual carboxylic acids in PGS.

Quantification of residual PVA in the final product is difficult due to the chemical similarity to PGS. Non-crosslinked pPGS-PVA fibers show characteristics of both PVA (broad alcohol peak at 3300-3500 cm^{-1}) and pPGS (alkane at 2800-3000, carbonyl at 1750 and 1700, and carbon-oxygen bond at 1000-1300 cm^{-1}). FTIR results for PGS-PVA fibers and PGS films show very similar spectra with the largest difference being the broad alcohol peak remaining

in the fibrous sample. In the C1 fibers, and less noticeably in the C5 group, washing the samples shifts the alcohol peak to higher wavenumber like that of the PGS. DSC was also performed to further elucidate the PVA content. PVA has a melting point of 165°C and crystallization temperature of 135°C that appeared in both PGS-PVA samples regardless of purification. FTIR and DSC results are in agreement with mass measurements, suggesting that residual PVA increases with degree of crosslinking and that washing steps are effective for removing some PVA from all groups.

Successful purification should also remove uncrosslinked pPGS. In the FTIR spectrum, the pPGS peak around 1700cm^{-1} [30] significantly shrinks after washing. DSC shows a melting point of 10°C for pPGS that shifted down to around −10°C as crosslinked to PGS [31]. PGS-PVA fibers for both crosslinking conditions exhibit this crosslinking-dependent shift of the Tm(PGS). DSC profiles of the purified fiber samples are shifted to closely match the multi-peak profiles for PGS film controls. This demonstrates the removal of substantial pPGS from the fibrous samples during purification.

3.4 Mechanical properties

Uniaxial tensile testing of hydrated samples was performed to evaluate the effect of three different crosslinking regimens on tensile properties. Samples were strained perpendicular and parallel to the electrospinning mandrel axis, although the orientation exhibited little effect on results. All samples demonstrated approximately 1 MPa of ultimate tensile strength (UTS) regardless of crosslinking (**Figure 4a**). As the degree of crosslinking increased, the modulus increased from 100 to 800 kPa while the strain to failure (STF) decreased from 800% to 200%. Elasticity was measured by performing a 100-cycle multi-cycle testing between 10 and 100% strain. The most crosslinked sample (C5) showed full recovery back to 10% strain while absorbing energy during the first cycle (**Figure 4c**). This recovery and energy loss matches behavior previously reported for PGS alone [32, 33]. All groups exhibited suture retention. However, as moduli increased, the samples deformed less and were more susceptible to tearing as demonstrated by the lowest suture retention strength (SRS) of C5.

PGS is a desirable material for soft tissue replacement because of the modulus in the kPa range similar to tissues. Despite the possible presence of residual PVA, the fibrous PGS sheets exhibited similar moduli to reported values for porous (106-125μm pores) and nonporous PGS (**Figure 4b**) [16] while demonstrating 5 times greater strength and 3 to 8 times larger strain-to-failure. As a biorubber, PGS can be elongated several times its original length and is elastic during cyclic testing. Furthermore, we demonstrate that mechanical properties can still be tuned by adjusting the degree of crosslinking. Most importantly for clinical translation, we believe that this is the first report of suturable PGS scaffolds (**Supplementary video 1**). The inability to hold suture was a significant shortcoming of salt-leached PGS scaffolds (data not shown) and a leading motivation for this work. To implant salt-leached PGS vascular grafts, our laboratory has previously applied a mechanically reinforcing PCL sheath to improve the graft's suture retention, but reinforced grafts still required gentle surgical handling [6].

The elasticity of our electrospun PGS scaffolds distinguishes it from those produced in other reports. Electrospun PGS blended with polyesters yields stiff constructs due to the presence of the carrier polymer. For PGS that was coaxially spun with PLLA, no mechanical data was reported after PLLA removal, but with PLLA present, strain to failure is one tenth that of PGS, and Young's modulus is 300 times stiffer [34]. Mechanical properties of PCL-PGS blends were closer to that of PCL itself than PGS elastomer [24]. Gelatin blends closely match PGS mechanical properties when hydrated, but differ by several orders of magnitude when dried. Additionally, results of our PGS-gelatin blends (not published) showed poor suture retention.

The suitability of electrospun PGS for various applications is determined largely by their required mechanical properties. For instance, scaffolds with lower crosslinking conditions are more elastic and more appropriate for cyclic loading-unloading conditions such as in blood vessels. In contrast, more crosslinked scaffolds hold their shape under mechanical forces but tear more easily. These may be useful for less dynamic applications such as nerve regeneration.

3.5 Cytocompatibility and in vivo host response

We hypothesized that the purified product would have similar cytocompatibility to thermally-crosslinked PGS since no chemical crosslinkers were added. Additionally, since PGS was crosslinked, the scaffolds were washed in ethanol to remove residual monomers and oligomers which are believed to harm cells if not removed [9, 25]. Furthermore, the wash steps are performed in water and ethanol, avoiding harsh organic solvents.

Live/Dead staining for 3T3 cells in direct contact with the PGS sheets (**Figure S3**) demonstrated the presence of live cells (green) but could not distinguish dead cells (red) due to autofluorescence of the PGS fibers (red). Extracts were added to 3T3 cells on TCPS to evaluate the effect of different crosslinking and purification conditions. Results were quantified by Live/Dead staining and normalized to no extract controls (**Figure 5a**). None of the purified samples exhibited any difference from solvent casted PGS films, suggesting that electrospun PGS fibers have similar cytocompatibility to PGS film. Only the non-purified C1 group at 10mg/mL demonstrated significant difference from the control. As previously reported, the least crosslinked group has the most residual monomer and greatest effect on cell viability.[9, 25] However, this effect disappears after washing, suggesting the effectiveness and importance of purification after forming PGS. Furthermore, fibrous PGS showed no significant effect on the viability of hcbECs compared with PLGA controls, suggesting minimal metabolic effects from residual PVA **(Figure 5b)**. In agreement with previous observations [15], cells attach to sheets of PGS fibers with morphology that varies from round to elongated (**Figure 5c**) as substrate stiffness is increased [35, 36].

Gross analysis **(Figure 6 a-d)** of the subcutaneous implants indicates the presence of the polymer at both 3 and 14 days. H&E images at day 3 **(Figure 6 e&f)** revealed substantial neutrophil infiltration surrounding both PGS and PLGA samples that extended into the center of the implant. Scattered phagocytic macrophages were also observed throughout the samples. By day 14 substantial resorption of scaffolds implanted in both groups was evident by gross-inspection and inflammation had largely subsided**(Figure 6 g&f)**. The outer

margins of both implants were surrounded by collagen-rich matrix and multi-nucleated giant cells, while fibroblast-like cells were present within the bulk of the implants. Collagen deposition is highlighted by the blue regions in the Masson's trichrome images **(Figure 6 k&l)**. These results suggests that the body responds similarly to electrospun PGS as it does to electrospun PLGA within the subcutaneous environment. Although biodegradation of these samples was not evaluated, we anticipate that the degradation rate will be similar to that of porous PGS. Future work will assess the effects of degradation rate at later time points as well as application-specific remodeling.

3.6 Advantages of pPGS-PVA electrospinning

Electrospun pPGS-PVA offers advantages to both traditional porogen leached PGS fabrication and other PGS electrospinning approaches. This work was motivated by the need for stronger PGS scaffolds, specifically for vascular grafts. Tubular constructs fabricated by electrospinning pPGS-PVA around small mandrels produce mechanically-robust grafts (**Supplemental video 2**) that permit facile suturing, stretching, and bending (**Figure 7a**), which are important properties for successful clinical adoption. Furthermore, SEM of electrospun scaffolds reveal a fibrous cross-section and uniform wall thickness (**Figure 7b&c**). In our experience, electrospinning PGS grafts is less labor-intensive but yields stronger, more reproducible products than salt leaching [8, 37, 38].

Our method also offers several key advantages to existing PGS electrospinning approaches: 1) The elasticity and relatively low modulus are retained. These mechanical properties are unique features of PGS that provide cells with the mechanical stimuli to promote elastin formation. This elastic behavior requires the cross-linking of pPGS to PGS as well as the removal of the carrier polymer that alters mechanical properties. 2) The use of potentially toxic components is limited to HFIP that is used as the solvent for most electrospinning. This is removed by evaporation during electrospinning, vacuum and heat during crosslinking, as well as multiple water and ethanol wash steps. Crosslinking with heat avoids the addition of substances with known toxicity such as glutaraldehyde and acrylates [39, 40]. Noncrosslinked pPGS and free monomers which may be harmful are removed via washes in ethanol, a benign solvent. The PVA removal in water is also nontoxic. 3) The technique is inexpensive. The PVA used as a carrier polymer costs significantly less than other frequently-used polymers (e.g. gelatin, PCL, PLLA). The use of standard pPGS avoids the cost of chemical modifications (e.g. pPGS-acrylate).

When properly controlled, PGS fiber fusion can be used to affix one layer of PGS to one another to produce multi-layered structures. This is demonstrated in **Figure 8a** where fibrous pPGS-PVA sheets were stacked and crosslinked between Teflon blocks. The mild fusion that occurs between fibers helps bond together multi-laminate fibrous scaffolds with indistinguishable layers (**Figure 8 b&c)**. Constructs resisted delamination by the T-peel test (**Figure 8 d-f**) which demonstrated the ability of this layer-layer interface to withstand nearly 10mN/mm peeling force. The layer-layer adhesion was increased if the second layer was directly electrospun onto the first. This difference likely results from additional solvent remaining in the directly electrospun layer, causing these fibers to solvent bond to the first layer even before crosslinking. Multi-laminate stacking presents a method to quickly obtain

tall electrospun scaffolds that would otherwise take very long time to electrospin the same thickness. The ability to laminate individual layers of fibers also offers great control of scaffold architecture (eg. random fibers on one side and aligned fibers on the other or layers of alternating fiber orientation). Finally, we envision customizing the pattern of each layer to create complex 3D objects by using similar methods to the rapid prototyping method of laminated object manufacturing (LOM). Existing use of LOM for tissue engineering applications is very limited, presenting a large opportunity for this technology.

3.7 Limitations and future work

There are several limitations to the work presented. As evidenced by **Figure 3**, not all PVA is removed in the final product. While we do not believe that this will significantly affect cellular response, we will pursue methods to improve PVA removal and further characterize the effects of residual PVA. A second challenge is obtaining sufficient porosity within our electrospun scaffolds. Tight fiber packing is common for most electrospinning and is known to limit cell infiltration [41, 42]. This problem may be exacerbated for our scaffolds due to the fiber fusion, especially on solid surfaces such as the mandrel (**Figure 7c**). A previous study that cultured smooth muscle cells (SMC) on porous PGS scaffolds reported 25-32 μm pore size to be optimal for SMC infiltration and elastin synthesis [8]. Thus, incorporating pores of this size will be the focus of future work in vascular applications. The morphological differences that result from varied crosslinking conditions will also be investigated. We anticipate that the non-cylindrical fibers will weaken mechanical properties but may improve cell adhesion to the textured surfaces.

4. Conclusion

We developed a simple method for electrospinning PGS using standard electrospinning apparatus and nontoxic carrier polymer, PVA. This approach offers advantages over other scaffold fabrication methods, such as solvent casting porogen leaching, by producing mechanically strong and fibrous scaffolds. Additionally, it avoids many of the cytotoxicity concerns associated with the crosslinking and purification techniques used in previous electrospinning strategies for PGS. This technique provides a new tool for processing PGS into scaffolds with more robust handling for surgical implantation. The mechanical strength, notably suture retention, is much higher than porogen leached scaffolds. Additionally, electrospun PGS should enable rapid and economical scale-up and more reliable manufacturing compared to salt-leaching methods. Thus, this work should accelerate clinical translation of PGS.

Supplementary Material

Refer to Web version on PubMed Central for supplementary material.

Acknowledgements

We thank Dr. Edwin Klein for his assistance in interpreting the host response to implanted scaffolds. We would also like to thank Dr. Kee-won Lee for providing data for the T-peel tests. Research reported in this publication was supported by the National Heart, Lung, and Blood Institute of the National Institutes of Health under award number HL089658-07. The content is solely the responsibility of the authors and does not necessarily represent the official views of the National Institutes of Health.

References

1. Engler AJ, Sen S, Sweeney HL, Discher DE. Matrix elasticity directs stem cell lineage specification. Cell. 2006; 126(4):677–89. [PubMed: 16923388]
2. Discher DE, Janmey P, Wang YL. Tissue cells feel and respond to the stiffness of their substrate. Science. 2005; 310(5751):1139–43. [PubMed: 16293750]
3. Sabir MI, Xu X, Li L. A review on biodegradable polymeric materials for bone tissue engineering applications. Journal of Material Science. 2009; 44:5713–24.
4. Li Y, Thouas GA, Chen Q-Z. Biodegradable soft elastomers: synthesis/properties of materials and fabrication of scaffolds. Royal Society of Chemistry. 2012; 2:8229–42.
5. Rai R, Tallawi M, Grigore A, Boccaccini AR. Synthesis, properties and biomedical applications of poly(glycerol sebacate) (PGS): A review. Progress in Polymer Science. 2012; 37:1051–78.
6. Wu W, Allen RA, Wang Y. Fast-degrading elastomer enables rapid remodeling of a cell-free synthetic graft into a neoartery. Nat Med. 2012; 18(7):1148–53. [PubMed: 22729285]
7. Crapo PM, Wang Y. Physiologic compliance in engineered small-diameter arterial constructs based on an elastomeric substrate. Biomaterials. 2010; 31(7):1626–35. [PubMed: 19962188]
8. Lee KW, Stolz DB, Wang Y. Substantial expression of mature elastin in arterial constructs. Proc Natl Acad Sci U S A. 2011; 108(7):2705–10. [PubMed: 21282618]
9. Chen QZ, Ishii H, Thouas GA, Lyon AR, Wright JS, Blaker JJ, et al. An elastomeric patch derived from poly(glycerol sebacate) for delivery of embryonic stem cells to the heart. Biomaterials. 2010; 31(14):3885–93. [PubMed: 20153041]
10. Engelmayr GC Jr. Cheng M, Bettinger CJ, Borenstein JT, Langer R, Freed LE. Accordion-like honeycombs for tissue engineering of cardiac anisotropy. Nat Mater. 2008; 7(12):1003–10. [PubMed: 18978786]
11. Radisic M, Marsano A, Maidhof R, Wang Y, Vunjak-Novakovic G. Cardiac tissue engineering using perfusion bioreactor systems. Nat Protoc. 2008; 3(4):719–38. [PubMed: 18388955]
12. Sundback CA, Shyu JY, Wang Y, Faquin WC, Langer RS, Vacanti JP, et al. Biocompatibility analysis of poly(glycerol sebacate) as a nerve guide material. Biomaterials. 2005; 26(27):5454–64. [PubMed: 15860202]
13. Redenti S, Neeley WL, Rompani S, Saigal S, Yang J, Klassen H, et al. Engineering retinal progenitor cell and scrollable poly(glycerol-sebacate) composites for expansion and subretinal transplantation. Biomaterials. 2009; 30(20):3405–14. [PubMed: 19361860]
14. McKee CT, Last JA, Russell P, Murphy CJ. Indentation versus tensile measurements of Young's modulus for soft biological tissues. Tissue engineering Part B, Reviews. 2011; 17(3):155–64. [PubMed: 21303220]
15. Wang Y, Ameer GA, Sheppard BJ, Langer R. A tough biodegradable elastomer. Nat Biotechnol. 2002; 20(6):602–6. [PubMed: 12042865]
16. Mitsak AG, Dunn AM, Hollister SJ. Mechanical characterization and non-linear elastic modeling of poly(glycerol sebacate) for soft tissue engineering. J Mech Behav Biomed Mater. 2012; 11:3–15. [PubMed: 22658150]
17. Billiet T, Vandenhaute M, Schelfhout J, Van Vlierberghe S, Dubruel P. A review of trends and limitations in hydrogel-rapid prototyping for tissue engineering. Biomaterials. 2013; 33(26):6020–41. [PubMed: 22681979]
18. Finne-Wistrand A, Albertsson AC, Kwon OH, Kawazoe N, Chen G, Kang IK, et al. Resorbable scaffolds from three different techniques: electrospun fabrics, salt-leaching porous films, and smooth flat surfaces. Macromol Biosci. 2008; 8(10):951–9. [PubMed: 18567051]
19. Ashammakhi N, Ndreu A, Nikkola L, Wimpenny I, Yang Y. Advancing tissue engineering by using electrospun nanofibers. Regen Med. 2008; 3(4):547–74. [PubMed: 18588476]
20. Bettinger CJ. Biodegradable elastomers for tissue engineering and cell-biomaterial interactions. Macromol Biosci. 2011; 11(4):467–82. [PubMed: 21229578]
21. Chaouat M, Le Visage C, Baille WE, Escoubet B, Chaubet F, Mateescu MA, et al. A novel cross-linked poly(vinyl-alcohol) (PVA) for vascular grafts. Advanced Functional Materials. 2008; 18(2855-2861)

22. Hassan CM, Peppas NA. Structure and applications of Poly(vinyl alcohol) hydrogels produced by conventional crosslinking or by freezing/thawing methods. Advances in Polymer Science. 2000; 153:37–65.
23. Yi F, LaVan DA. Poly(glycerol sebacate) nanofiber scaffolds by core/shell electrospinning. Macromol Biosci. 2008; 8(9):803–6. [PubMed: 18504802]
24. Sant S, Hwang CM, Lee SH, Khademhosseini A. Hybrid PGS-PCL microfibrous scaffolds with improved mechanical and biological properties. J Tissue Eng Regen Med. 2010
25. Li Y, Cook WD, Moorhoff C, Huang W-C, Chen Q-Z. Synthesis, characterization and properties of biocompatible poly(glycerol sebacate) pre-polymer and gel. Polymer international. 2013; 62:534–47.
26. Ifkovits JL, Devlin JJ, Eng G, Martens TP, Vunjak-Novakovic G, Burdick JA. Biodegradable fibrous scaffolds with tunable properties formed from photo-cross-linkable poly(glycerol sebacate). ACS Appl Mater Interfaces. 2009; 1(9):1878–86. [PubMed: 20160937]
27. Ravichandran R, Venugopal JR, Sundarrajan S, Mukherjee S, Ramakrishna S. Poly(Glycerol sebacate)/gelatin core/shell fibrous structure for regeneration of myocardial infarction. Tissue Eng Part A. 2011; 17(9-10):1363–73. [PubMed: 21247338]
28. Liu T, Teng WK, Chan BP, Chew SY. Photochemical crosslinked electrospun collagen nanofibers: synthesis, characterization and neural stem cell interactions. J Biomed Mater Res A. 2010; 95(1): 276–82. [PubMed: 20607867]
29. Ruder C, Sauter T, Kratz K, Haase T, Peter J, Jung F, et al. Influence of fibre diameter and orientation of electrospun copolyetheresterurethanes on smooth muscle and endothelial cell behaviour. Clinical hemorheology and microcirculation. 2013; 55(4):513–22. [PubMed: 24113506]
30. LeBlon CE, Pai R, Fodor CR, Golding AS, Coulter JP, Jedlicka SS. In Vitro Comparative Biodegradation Analysis of Salt-Leached Porous Polymer Scaffolds. Journal of Applied Polymer Science. 2012
31. Jaafar IH, Ammar MM, Jedlicka SS, Pearson RA, Coulter JP. Spectroscopic evaluation, thermal, and thermomechanical characterization of poly(glycerol-sebacate) with variations in curing temperatures and durations. Journal of Material Science. 2010; 45:2525–9.
32. Patel A, Gaharwar AK, Iviglia G, Zhang H, Mukundan S, Mihaila SM, et al. Highly elastomeric poly(glycerol sebacate)-co-poly(ethylene glycol) amphiphilic block copolymers. Biomaterials. 2013; 34(16):3970–83. [PubMed: 23453201]
33. Liang SL, Cook WD, Thouas GA, Chen QZ. The mechanical characteristics and in vitro biocompatibility of poly(glycerol sebacate)-bioglass elastomeric composites. Biomaterials. 2010; 31(33):8516–29. [PubMed: 20739061]
34. Xu B, Rollo B, Stamp LA, Zhang D, Fang X, Newgreen DF, et al. Non-linear elasticity of core/shell spun PGS/PLLA fibres and their effect on cell proliferation. Biomaterials. 2013; 34(27): 6306–17. [PubMed: 23747009]
35. Marsano A, Maidhof R, Wan LQ, Wang Y, Gao J, Tandon N, et al. Scaffold stiffness affects the contractile function of three-dimensional engineered cardiac constructs. Biotechnol Prog. 2010; 26(5):1382–90. [PubMed: 20945492]
36. Yeung T, Georges PC, Flanagan LA, Marg B, Ortiz M, Funaki M, et al. Effects of substrate stiffness on cell morphology, cytoskeletal structure, and adhesion. Cell Motil Cytoskeleton. 2005; 60(1):24–34. [PubMed: 15573414]
37. Gao J, Crapo PM, Wang Y. Macroporous elastomeric scaffolds with extensive micropores for soft tissue engineering. Tissue Eng. 2006; 12(4):917–25. [PubMed: 16674303]
38. Crapo PM, Gao J, Wang Y. Seamless tubular poly(glycerol sebacate) scaffolds: high-yield fabrication and potential applications. J Biomed Mater Res A. 2008; 86(2):354–63. [PubMed: 17969024]
39. Jayakrishnan A, Jameela SR. Glutaraldehyde as a fixative in bioprostheses and drug delivery matrices. Biomaterials. 1996; 17(5):471–84. [PubMed: 8991478]
40. Yoshii E. Cytotoxic effects of acrylates and methacrylates: relationships of monomer structures and cytotoxicity. J Biomed Mater Res. 1997; 37(4):517–24. [PubMed: 9407300]

41. Dvir T, Timko BP, Kohane DS, Langer R. Nanotechnological strategies for engineering complex tissues. Nat Nanotechnol. 2010; 6(1):13–22. [PubMed: 21151110]

42. Stankus JJ, Guan J, Fujimoto K, Wagner WR. Microintegrating smooth muscle cells into a biodegradable, elastomeric fiber matrix. Biomaterials. 2006; 27(5):735–44. [PubMed: 16095685]

43. Sant S, Iyer D, Gaharwar AK, Patel A, Khademhosseini A. Effect of biodegradation and de novo matrix synthesis on the mechanical properties of valvular interstitial cell-seeded polyglycerol sebacatepolycaprolactone scaffolds. Acta Biomater. 2013; 9(4):5963–73. [PubMed: 23168222]

44. Kharaziha M, Nikkhah M, Shin SR, Annabi N, Masoumi N, Gaharwar AK, et al. PGS:Gelatin nanofibrous scaffolds with tunable mechanical and structural properties for engineering cardiac tissues. Biomaterials. 2013; 34(27):6355–66. [PubMed: 23747008]

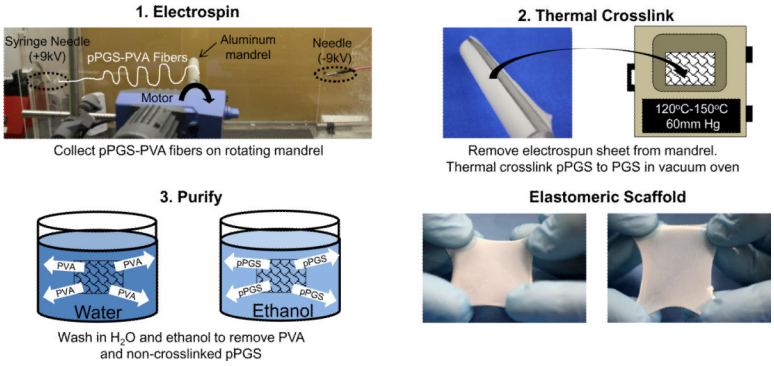

Figure 1.

Fabrication of fibrous PGS sheets. 1. Electrospin pPGS-PVA to rotating (100rpm) mandrel 30cm from syringe needle at (+9kV), and 30cm from negatively- charged needle (−9kV). 2. Crosslink the sheet with high temperate and vacuum. 3. Purify samples by washing in water for 24h to remove soluble PVA. Rinse in graded ethanol dilutions to remove non-crosslinked pPGS.

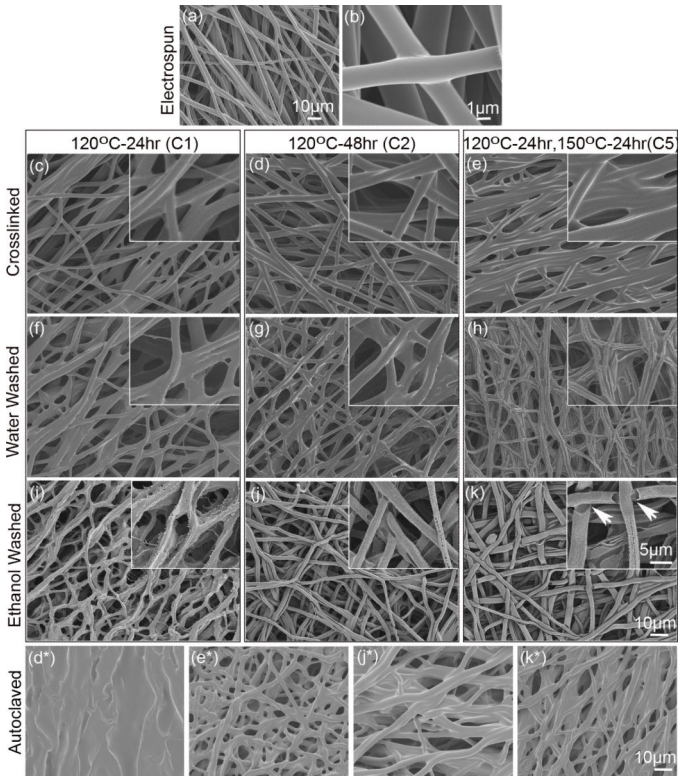

Figure 2.

SEM of PGS-PVA (55:45) fibers after electrospinning, thermal crosslinking, and purification. (a-b) Electrospun pPGS-PVA fibers. (c-e) PGS-PVA after crosslinking at respective conditions. (f-h) PGS-PVA fibers after washing in water for 24h. (i-k) PGS-PVA after ethanol purification. Inset: high magnification images of fibers. (*) Corresponding samples (d, e, j, k) after autoclaving. (Scale bar: 10μm for a, c-k and *; 5μm for all insets)

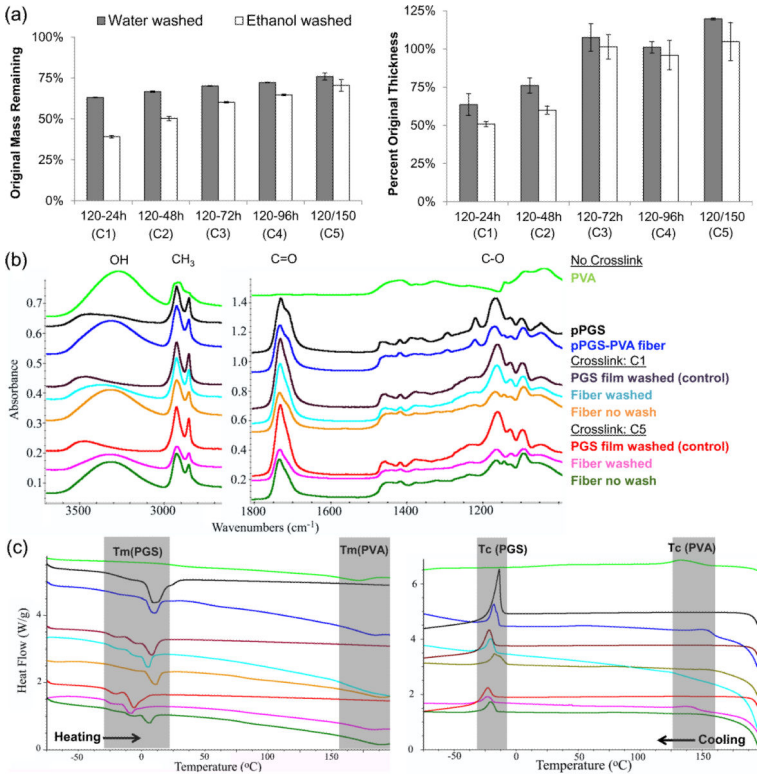

Figure 3.

Purification analysis. (a) Percent of unwashed mass and thickness remaining after water and ethanol washes for each crosslinking conditions. (b) ATR-FTIR spectra of PVA, PGS and PGS-PVA during purification. (c) Heating and cooling curves from DSC measurements. Colors use the same legend as (b).

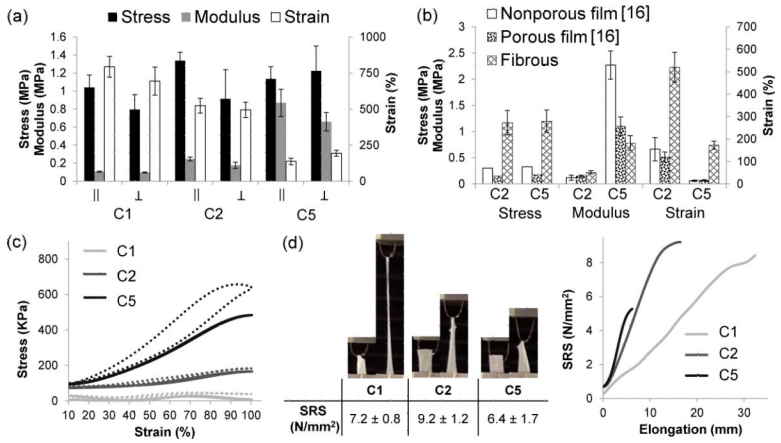

Figure 4.

Mechanical testing. (a) Tensile testing plot of samples strained parallel (||) or perpendicular (⊥) to fiber axis. (b) Comparison of fibrous PGS to previously reported mechanical properties for porous and non-porous films under similar conditions. Note: UTS values for nonporous and porous films was during testing of dry samples. C2 crosslinking was 120°C for all samples. C5 crosslinking for porous and nonporous films was 150°C-48h but 120°C-24h, 150°C-24h for fibers. (c) Multi-cycle testing of C5 sample, strained 10-100% for 100 cycles. (d) Suture retention strength.

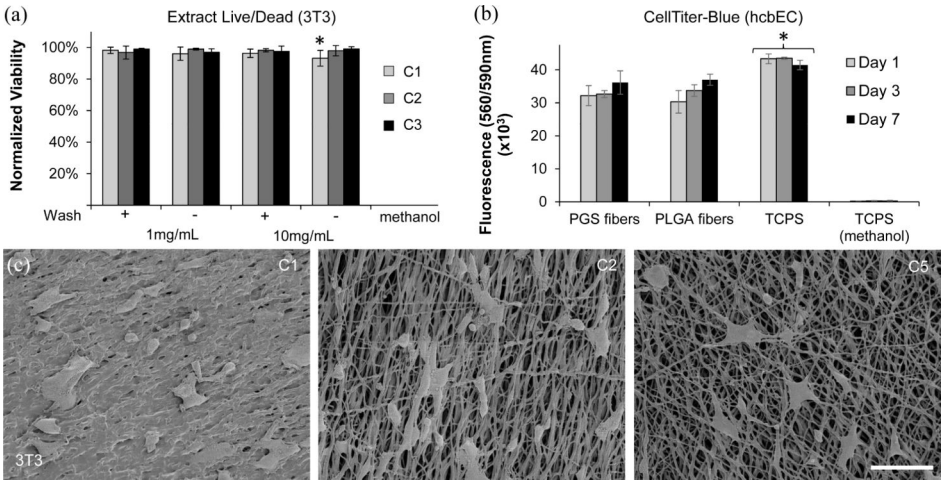

Figure 5.

Cytocompatibility of PGS-PVA fibers. (a) Normalized viability of 3T3 cells cultured with extract from PGS-PVA samples. (b) CellTiter-Blue cell viability colorimetric assay with hcbEC. Metabolic activity of cells was measured by fluorescence emission at 590nm after 560nm excitation. All groups were significantly different from TCPS controls (asterisk). PGS fibers were not significantly different from PLGA fibers. (c) SEM of 3T3 cells on PGS-PVA fibers. Scale: 100 μm

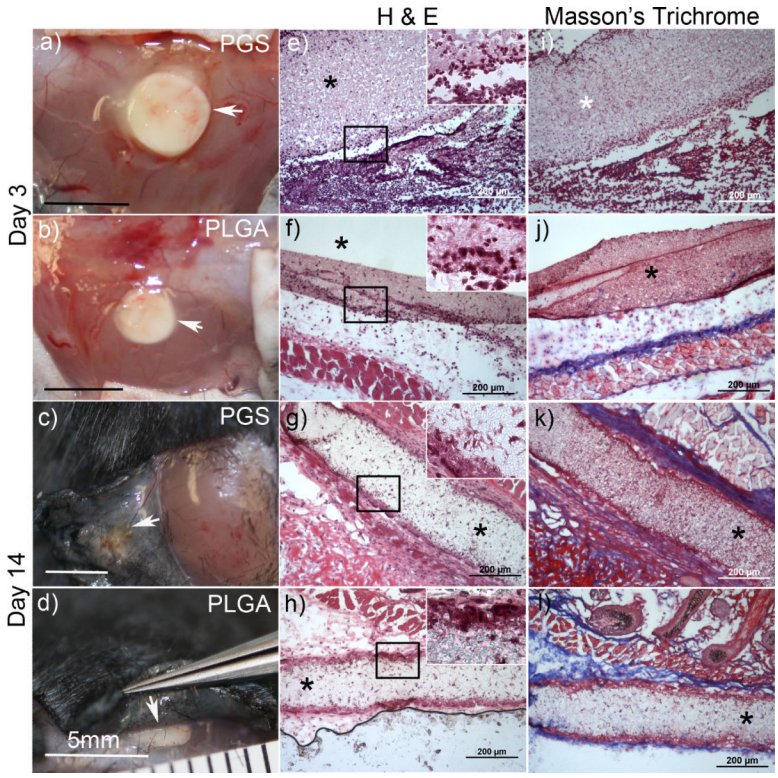

Figure 6.

Gross and histological images of fibrous PGS and PLGA implants after 3 and 14 days. Implants are indicated by arrowheads in gross images (a-d) of the subcutaneous tissue. Cross-sectional images stained by (H&E) are shown in (e-h) and Masson's trichrome (i-l) with implants indicated by an asterisk.

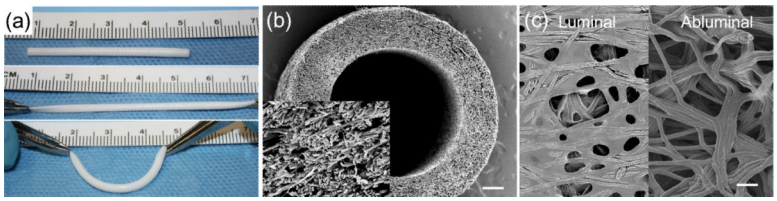

Figure 7.

PGS-PVA fibrous conduits. (a) Small-diameter conduits demonstrate elastic properties and easy handling. (b) The fibrous morphology of these conduits can be observed in the SEM cross-section (Scale: 200 μm, Insert: 20 μm). (c) SEM images of the luminal and abluminal surfaces of the conduit reveal fibers with some fusion around the mandrel. (Scale: 10 μm)

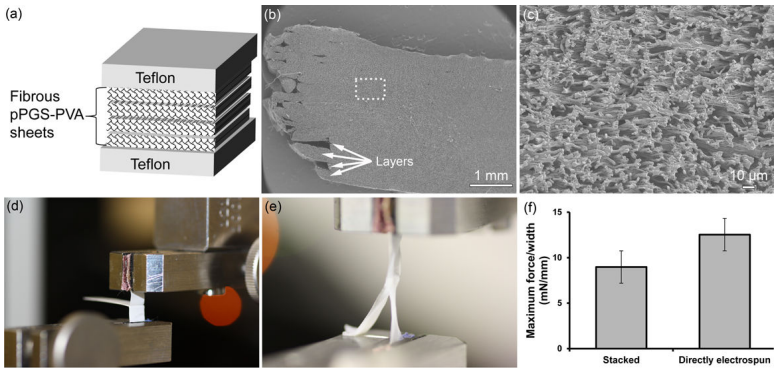

Figure 8.

Multi-laminate scaffolds. (a) Fibrous pPGS-PVA sheets were stacked between Teflon blocks and then thermally crosslinked. (b) SEM of purified multi-laminate structures reveals thick scaffolds with indistinguishable layers and (c) fibrous microstructure. (d) Image of dry laminated PGS sample in MTS grips before T-peel test. (e) Image of hydrated laminated PGS sample undergoing tensile T-peel testing. The free ends of the sample elongate while the two layers remain bonded together. (f) T-peel test maximum force/thickness before failing. Stacked samples were electrospun separately and laminated by stacking during crosslinking. In contrast, for directly electrospun samples, the second layer was electrospun onto the first layer.

Table 1

Review of PGS electrospinning. Cells highlighted in blue meet our criteria of standard electrospinning, thermal crosslinking, and removal of carrier polymer. Cells highlighted in green match mechanical property with that of previously reported thermal-crosslinked PGS.

Carrier Polymer	*i.* Electrospin Method	*ii.* Crosslink Method	*iii.* Carrier Removal	*UTS (MPa)*	*Strain (%)*	*Modulus (MPa)*
PLLA (2008) [23]	Core-sheath	Thermal	DCM	-	-	-
PLLA (2013) [34]	Core-sheath	Thermal	X	0.6-1.2	25	12
PCL (2013) [43]	Standard	X	X	3.5	-	7
PCL (2010) [24]	Standard	X	X	1.7-2.5	400-500	9-35
Gelatin (2009) [26]	Standard	Acrylate (UV)	X	0.05	30-40	0.1 to 1
Gelatin (2011) [27]	Core-sheath	Glutar-aldehyde	X	2*	61*	6*
Gelatin (2013) [44]	Standard	EDC-NHS	X	0.3-1	182-229	0.14-0.36
PCL	Standard	X	X			
PLGA	Standard	Isocyanate	THF			
PDO	Standard	Thermal	X			
Gelatin	Standard	Thermal	X			
PET	Standard	Thermal	HFIP			
PVA	Standard	Thermal	H_2O	0.8-1.3	200-800	0.1-0.8
PGS Film (Thermal-crosslinked) [5]				>0.5	>330	0.025-1.2

*Mechanical testing performed at dry state.